J. Iran. Chem. Soc., Vol. 4, No. 3, September 2007, pp. 279-298.

JOURNAL OF THE
Iranian
Chemical Society

Experimental and Theoretical Study on the Kinetics and Mechanism of Thermal Decomposition of 1,2-Dichloroethane

S.H. Mousavipour*, V. Saheb, F. Pirhadi and M.R. Dehbozorgi[a]
Department on Chemistry, College of Sciences, Shiraz University, Shiraz, Iran
[a]*Department of electrical Engineering, School of Engineering, Shiraz University, Shiraz, Iran*

(Received 11 October 2006, Accepted 8 December 2006)

The kinetics and mechanism for the thermal decomposition of 1,2-dichloroethane (EDC) was studied in a flow system over the temperature range of 849-1064 K and pressure range of 10-300 Torr under homogeneous conditions in a tubular quartz reactor. Gas chromatography was used to measure the concentration of products. Four-center HCl elimination was found to be the most important channel in this system. Minor products such as methane, ethylene, acetylene, chloroethane, and chloroprene were identified. *Ab initio* calculations at the DFT, CASMP2, and QCISD(T) levels of theory were carried out to investigate the mechanism of this system and to calculate necessary parameters to compute the rate constants of different steps. Dependence of formation of vinyl chloride on the total pressure is measured, experimentally.

Keywords: Kinetics and mechanism, Thermal decomposition, 1,2-Dichloroethane, Experimental, Pressure effect, *Ab initio* calculations

INTRODUCTION

1-2 Dichloroethane (EDC) is known as the major precursor for the formation of vinylchloride monomer (VCM) which is an industrially important chemical. The kinetics of this system has been studied by many researchers during the past 50 years [1]. The main reaction path for the decomposition of chlorinated ethane is reported as HCl elimination [1b]. Although, this reaction was studied by different groups, the temperature dependency of the corresponding rate constants with pressure has not been well defined. A chain reaction mechanism for the pyrolysis of EDC at low conversion might be proposed as

$CH_2ClCH_2Cl \rightarrow CH_2=CHCl + HCl$ R1

$CH_2ClCH_2Cl \rightarrow C_2H_4 + Cl_2$ R2

$CH_2ClCH_2Cl \rightarrow C_2H_4Cl + Cl$ R3

$C_2H_4Cl \rightarrow C_2H_4 + Cl$ R4

$CH_2ClCH_2Cl \rightarrow 2CH_2Cl$ R5

$CH_2=CHCl \rightarrow C_2H_2 + HCl$ R6

$CH_2Cl + CH_2ClCH_2Cl \rightarrow CH_3Cl + CH_2ClCHCl$ R7

$CH_2Cl + CH_2ClCH_2Cl \rightarrow CH_2Cl_2 + C_2H_4Cl$ R8

$CH_2ClCHCl \rightarrow C_2H_3Cl + Cl$ R9

$C_2H_4Cl \rightarrow C_2H_3Cl + H$ R10

*Corresponding author. E-mail: mousavi@susc.ac.ir

$Cl + CH_2ClCH_2Cl \rightarrow HCl + C_2H_3Cl_2$ R11

$Cl + CH_2ClCH_2Cl \rightarrow Cl_2 + C_2H_4Cl$ R12

$Cl + C_2H_4Cl \rightarrow Cl_2 + C_2H_4$ R13

$C_2H_3Cl_2 \rightarrow C_2H_3Cl + Cl$ R14

$CH_2Cl + Cl \rightarrow CH_2Cl_2$ R15

$2Cl \rightarrow Cl_2$ R16

According to the above mechanism and our experimental and theoretical investigations, ethylene, acetylene, chloromethane, and dichloromethane are the minor products of decomposition of EDC at the initial stages of the pyrolysis. Two possible paths for the formation of ethylene are four centre Cl_2 elimination, reaction R2, or stepwise Cl elimination, reactions R3 and R4. Thus, it would be interesting to investigate the importance of reaction R2 or reactions R3 and R4 in the formation of ethylene. Another interesting aspect of this system is C-C bond breaking, which the amount of formation of chloromethane and dichloromethane, the products of reactions R7 and R8, are an indication for this process.

Holbrook *et al*. [2] pointed out that reaction R2 might be mainly auto-catalyzed by the surface reaction. Cardy *et al*. [3] studied the effect of laser radiation on the pyrolysis of EDC, theoretically. They reported a value of 332 kJ mol^{-1} for the ΔH^{o}_{298} of reaction R3. Zhu and Bozzelli [4] studied the kinetics of reaction R2 theoretically and suggested a non-linear Arrhenius plot for reaction R2. In their paper, they emphasized that reaction R2 is not important in the pyrolysis of EDC. According to their calculations, they concluded that Cl_2 molecular elimination channel is not important when compared with the C-Cl bond cleavage path. They reported that four centre Cl_2 elimination channel has similar barrier to the H elimination channel. They reported ΔH^{o} for reaction R3 in the range of 79.59-90.20 kJ mol^{-1}, depending on the level of calculations. They also reported the kinetic parameters for reaction R2 as $k_2 = 7.6 \times 10^{10}$ exp(-411.7 kJ mol^{-1}/RT) s^{-1} at the G3MP2 level of theory. Howlett [5] reported the Arrhenius parameters for reaction R3 as $k_3 = 1 \times 10^{13}$ exp(-292.9 kJ mol^{-1}/RT) s^{-1}. Salouhi *et al*. [6] studied the pyrolysis of EDC over the temperature range of 763-793 K. They reported that overall rate constant of disappearance of EDC is independent to the temperature and its value is reported equal to 1.3×10^{13} s^{-1}. Barat and Bozzeli [7] studied the kinetics of reaction R4 theoretically and reported its Arrhenius parameters as $k_4 = 3.9 \times 10^{13}$ exp(-90.8 kJ mol^{-1}/RT) s^{-1}. Decomposition of CH_2CH_2Cl to ethylene and chlorine atom, reaction R4, was studied by Knyazev *et al*. [8] over the temperature range of 400-480 K. They reported high pressure Arrhenius parameters for this reaction as $k_4 = 1.7 \times 10^{14}$ exp(-72.8 kJ mol^{-1}/RT) s^{-1}.

The other possible initiation reaction of EDC decomposition is carbon-carbon bond cleavage, reaction R5. Two main products from C-C cleavage in this system are methyl chloride and methylene chloride according to reactions R7 and R8. To the best of our knowledge, the kinetics of reaction R5 is not well established, although methyl chloride and methylene chloride are reported as byproducts in the pyrolysis of EDC [9].

Martens and Huybrechts [10] studied the effect of the number of chlorine atoms on dissociation energy of C-C bond cleavage in ethane. They showed that the initiation step in hexachloroethane is the cleavage of the C-C bond rather than C-Cl bond cleavage. They suggested that, in less chlorinated ethane, dissociation energy for a C-Cl bond cleavage is lower than that for C-C bond cleavage. We have previously studied the kinetics of the pyrolysis of methyltrichlorosilane (MTS), experimentally [11]. In that case, the most probable dissociation reaction path for MTS was also found to be the carbon-silicon cleavage rather than HCl elimination, which is the main path reaction in the decomposition of EDC. Song *et al*. [12] studied the kinetics and mechanism of pyrolysis of EDC over a temperature range of 573-873 K. They reported VCM as the major product and *cis*-dichloroethane, trans-dichloroethane, 1,1-dichloroethane and chloroprene as minor products. Choi *et al*. [13] studied the effect of CCl_4 on the pyrolysis of EDC. They considered 108 reversible elementary reactions for modeling the pyrolysis of EDC and reported VCM as the main source of formation of acetylene.

Rajakumar *et al*. [14] studied the HCl elimination from EDC behind reflected shock waves in a single pulse shock tube over the temperature range of 1071-1174 K, pressure range of 11.2-15.0 atm, and dwell time of 0.504-0.720 ms.

They reported VCM, acetylene, ethyl chloride, and ethylene as products. They did not make any comments on the mechanism for the formation of ethyl chloride in such a small reaction times. We suggest that ethyl chloride should be a secondary product in that system. Rajakumar and Arunan [15] in a theoretical work at the B3LYP/6-311++G(d,p) level studied the HF, HCl, and ClF elimination reactions from CH_2F-CH_2Cl. They reported Arrhenius expression for reaction R1 as $k_1 = 4.8 \times 10^{13} \exp(-244 \text{ kJ mol}^{-1}/RT) \text{ s}^{-1}$.

Hassler *et al*. [16] considered falloff behavior for reaction R1 and pointed out that, at 1.3 atm, this reaction is in high-pressure limit at 600-1500 K. Kara and Senkan [17] have analyzed the falloff behavior of $CH_2Cl + CH_2Cl$ from 0.5 atm up to 10 atm and T = 500-1700 K. They pointed out the lack of experimental data on the falloff behavior of reaction R1 and cautioned that their results await experimental verification. Incavo [9] studied 1,2-dichloroethane cracking to vinyl chloride in the presence of CCl_4 and Cl_2 at 500 K. He reported different byproducts including methyl chloride and methylene chloride. In his results, the amount of methyl chloride is comparable with the amount of acetylene at lower residence time. Acetylene is the product of HCl elimination from VCM. He also reported that the amount of produced ethylene (the product of Cl_2 elimination reaction) is much higher than the amount of produced acetylene. Seetula [18] reported bond strengths of different chlorinated ethanes and ethyl radicals in an *ab initio* study. He reported that the bond strength for C-C bond is 375.8 kJ mol^{-1}, for C-Cl bond is 338.9 kJ mol^{-1}, and for C-H bond is 407.3 kJ mol^{-1}. Cioslowski *et al*. [19] studied the thermochemistry of homolytic C-C, C-H, and C-Cl bond dissociation in polychloroethanes. They reported a value of 364.5 ± 13.8 kJ mol^{-1} for $\Delta H°$ of reaction R5.

The main purpose of the present study was to investigate the pressure dependency of formation of VCM and contribution of different paths for the formation of ethylene. To achieve this goal, we have done some theoretical calculations to explore the potential energy surfaces for different channels and calculating high pressure rate constants by means of transition state theory and RRKM method.

EXPERIMENTAL

1,2-Dichloroethane (EDC) (> 99% purity, b.p. = (83.5 °C), d_4^{20} = 1.23 g cm^{-3} and vapor pressure 79.1 mmHg at 25 °C) from Merck company was used in this study. Acetylene of 99% purity and chloroethane of 98% purity (Merck-Schuohardt) were used to prepare the calibration mixtures to measure the concentration of the products. VCM and methyl chloride were synthesized in our lab to make standard mixture for GC calibration. The concentrations in the standard mixtures for calibration were kept close to the concentration of different products, about 10^{-9}-10^{-4} M. Argon of 99% purity was used as bath gas in the reactor. The reactant was degassed three times before introducing into the system. The mixture of EDC vapor in argon was prepared by bobbling the argon into the degassed liquid EDC.

The flow system used for this study is shown in Fig. 1. In this system a 10 l bulb was used to store the vapor of the reactant (EDC) in Argon. A greaseless needle valve was used to control the flow rate into the reactor. To examine the possible surface reactions, two 80-cm-long cylindrical quartz reactors with different surface-to-volume ratios were used. The effective cross sections of reactors were 0.041 cm^2 and 0.140 cm^2. The effective surface-to-volume ratios (s/v) for these reactors were 17.5 cm^{-1} and 9.48 cm^{-1}, respectively. During the experiments, a 40-cm-long section of the two reactors with different cross sections was heated by a resistive horizontal furnace with the nichrome wire element. A programmable temperature controller was used to regulate the temperature of the reactor. The reactor temperature was monitored by a platinum/platinum-13%-rhodium thermocouple. These electronic equipments were made in our lab. The effective length and temperature of the reactor was calculated from experimental temperature profile using a FORTRAN program [20].

The average residence time of molecules in the reactor was calculated from the measured pressure, temperature, effective cross-section of the reactors, and the reactant flow rate. Two digital pressure transducers (Druck DPI 705) were used to control and monitor the pressure of the manifold before the reactor and in the reactor. A six-way linear stainless steel gas sampling valve at the exit of the reactor was used to take samples in a 10 cm^3 sample loop and inject the sample in to a gas chromatograph (GC) (Shimadzu GC-A8) with a flame ionization detector (FID) to analyze the organic compounds. The products were separated on a 2-m silica gel column (mesh

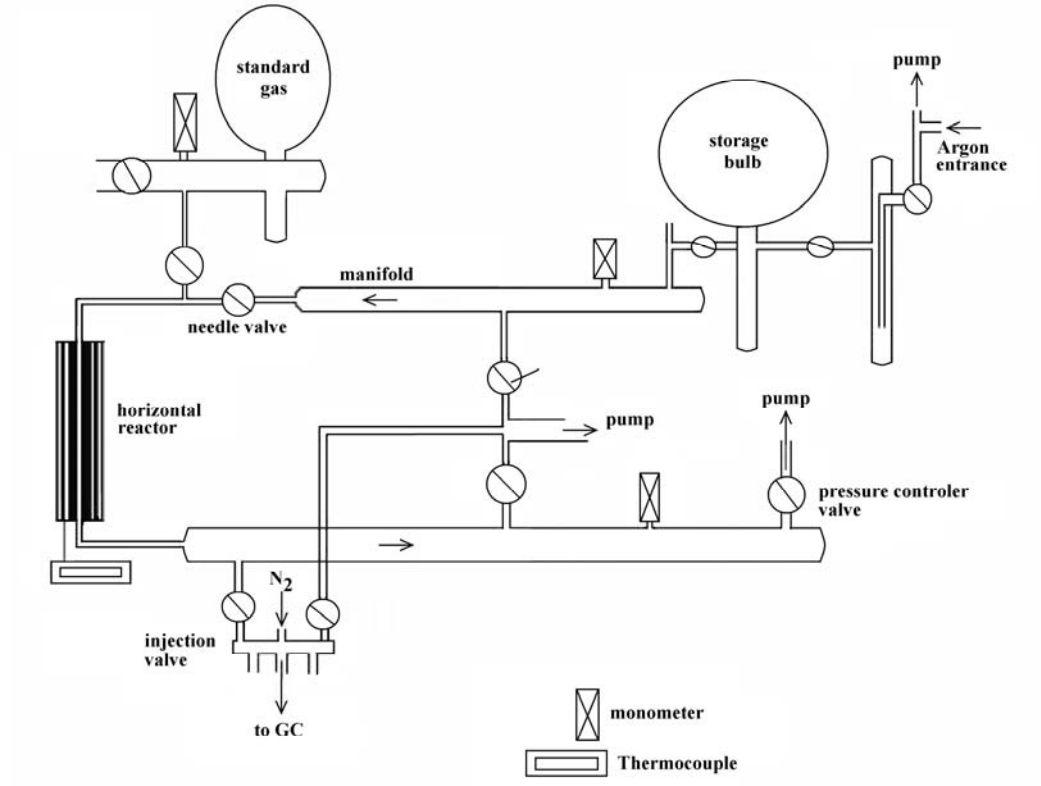

Fig. 1. Schematic diagram of the apparatus used for the study of pyrolysis of 1,2-dichloroethane.

35-70), using column temperature programming to achieve better separation of products. Nitrogen was used as carrier gas in GC.

Procedure

The EDC was degassed and distilled by condensing with liquid nitrogen. A flow of bath gas was bubbled through the liquid reactant and the mixture of reactant in Argon was placed in the storage bulb shown in Fig. 1. The partial pressure of EDC in Argon at the inlet of the reactor was measured by GC. Before each experiment, the EDC was degassed in liquid nitrogen again and checked for any impurity by analysis of the non reacted EDC in the gas chromatograph. There was not any measurable amount of impurities in the EDC.

The pressure of the EDC/Argon mixture in the storage bulb was kept constant and was controlled by maintaining an appropriate temperature of the storage bulb and controlling the Argon flow into the system. The grease-less needle valve was used to control the flow rate of the EDC/Argon mixture. At each flow conditions, several GC injections were made to take the average of GC peaks areas in calculating the concentrations of the products.

RESULTS

The reaction was studied over the temperature range of 825 ± 5 K to 1064 ± 5 K and the pressure range of 10 ± 2 to 300 ± 5 Torr using argon as bath gas. The major path in the pyrolysis of 1,2-dichloroethane was molecular dehydroclorination of EDC, reaction R1.

$$CH_2ClCH_2Cl \rightarrow C_2H_3Cl + HCl \qquad R1$$

At higher conversion regime (more than 15%) minor products like ethylene, acetylene, dichloroethane, chloroprene, methane, and chloromethane were observed. Quantitative

analysis of the products indicates that C-C bond fission reaction was not important in this process. Figure 2 shows the chordal rates (average rates) of formation of vinyl chloride, ethylene and acetylene in a specific condition (the chordal rates of formation of these products at different conditions are available on request). Each point in Fig. 2 is the average of at least three measurements. Steady-state rates of formation of the products were calculated from their average rates of formation in the plateau region in these Figures. Table 1 listed the steady-state rates of formation of different products at each pressure and temperature that measured in two reactors. As shown in Table 1, there was no trend evident in the steady-state rates of formation of different products on changing surface-to-volume ratio of the reactor, which means the surface reaction was not important in our experiments. Also in Table 1 we have shown the calculated rate constants for the formation of VCM at different conditions. In the first and second columns of Table 1 the total pressure of the mixture of the reactant plus argon and concentration of the reactant in the mixture is listed, respectively.

As shown in Table 1, we were just able to measure the concentration of ethylene and acetylene at higher temperatures of 946 and 1064 K. It is not apparent that the only source for the formation of ethylene, the primary byproduct, is 1,2-elimination of Cl_2 processes. Based on a theoretical study, Zhu and Bozzelli [4] proposed the rate constant for Cl_2 elimination from EDC as $7.62 \times 10^{10}\ T^{0.892}$ exp (-412.1 kJ mol^{-1}/RT) s^{-1}. The enthalpy changes for this reaction is $\Delta H° = 44.07$ kJ mol^{-1}. It was necessary to investigate this idea more carefully by performing theoretical calculations. These calculations are presented in the theoretical section of the present paper.

The average rates of formation of VCM are shown as R_{vc} in Table 1 and values of k_1 at different temperatures and pressures are listed in the last column of Table 1. Troe method [21] was used to calculate the falloff behavior for unimolecular rate constant k_1. In this study, Eq. (1) was fitted to the experimental data at different conditions by a nonlinear least squares procedure to estimate the low- and high-pressure limiting values for k_1.

$$k_1 / k_{1\infty} = F_{LH} F_c^{SC} F_c^{WC} \qquad (1)$$

where,

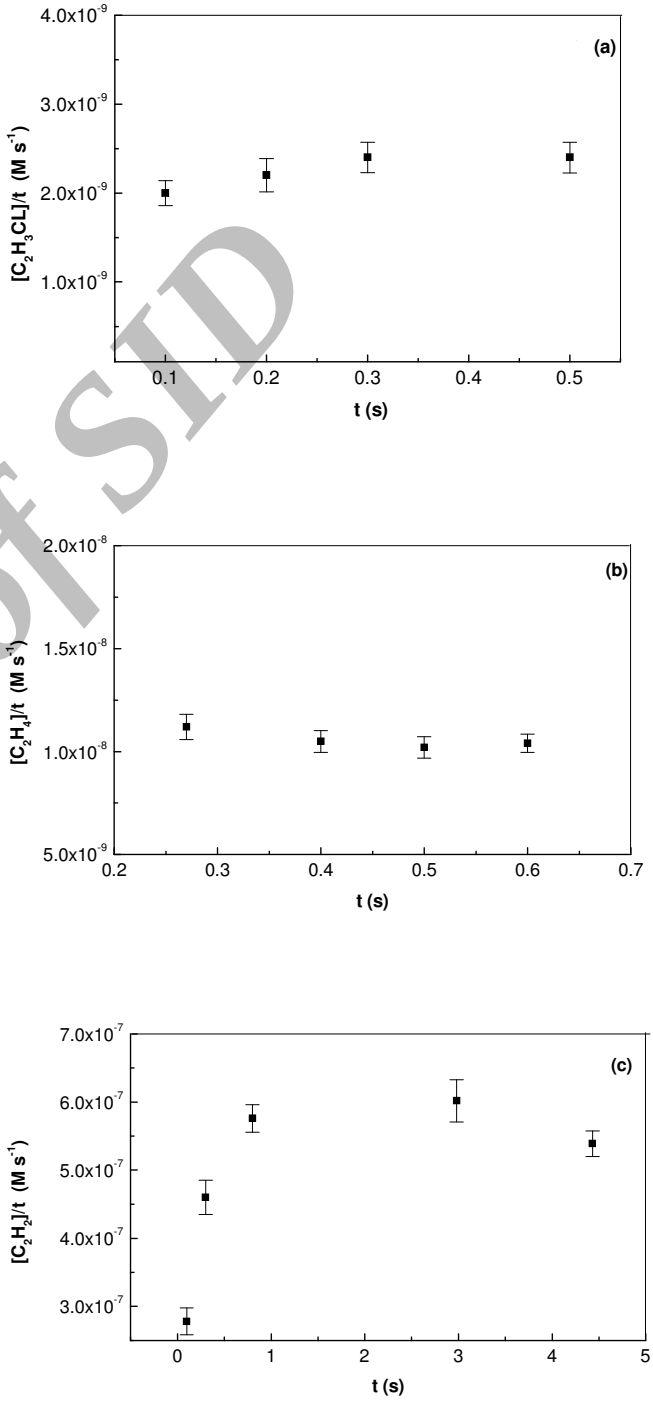

Fig. 2. Chordal rate of formation of vinyl chloride at 10 Torr and 849 K (a), ethylene at 300 Torr and 1064 K (b), and acetylene at 140 Torr and 1064 K (c) in reactor 2.

$$F_{LH} = \frac{k_{1,0}[M]/k_{1,\infty}}{1 + \frac{k_{1,0}[M]}{k_{1,\infty}}} \quad (2)$$

Here $k_{1,\infty}$ and $k_{1,0}$ are the limiting high- and low-pressure rate constants, respectively. The results showed that $k_{1,\infty}$ was not sensitive to the weak collision part of the expression, F^{WC}_{C}, and changing the collision efficiency from unity to 0.1 changed $k_{1,\infty}$ by only 10%. For these calculations, values of the Troe input parameters, S_k, B_T, and F_C^{SC} for reaction R1 were calculated at different temperatures and are listed in Table 2. The results of nonlinear least squares fitting are shown in Fig. 3 as solid lines. Points in Fig. 3 are experimental data at different temperatures. Arrhenius plot for reaction R1 at high pressure is shown in Fig. 4, which is compared with the reported values for k_1 in the literature. Linear least squares fitting to our data in Fig. 4 gave the following Arrhenius expression for $k_{1,\infty}$: $k_{1,\infty} = 4.2 \times 10^{13}$ exp(-235.7 kJ mol^{-1}/RT) s^{-1}.

In Table 1 are reported the average rate of formation of acetylene and ethylene at higher temperatures. Although, the other products like chloromethane and dichloromethane where measured qualitatively, it was difficult to measure these products quantitatively. A comparison between the effect of pressure on the rate of formation of VCM, acetylene, and ethylene in Table 1 reveals that the rate of formation of ethylene is much less affected by increasing the total pressure than the rate of formation of the two other products. These observations could be the reason that the only source for the formation of ethylene in this system is not just reaction R2, a unimolecular process, but its formation is the result of reaction R2 and also some other bimolecular reactions like reactions R12 and R13, the rate of which should not be affected by the pressure. For the formation of acetylene, we also noticed that pressure dependency was not adequate for a unimolecularity behavior. We assume that again some bimolecular step(s) like reaction R17 followed by reaction R18 should be involved in the formation of this byproduct and its consumption in reactions like reaction R19.

$$CH_2{=}CHCl + Cl \rightarrow CH{=}CHCl + HCl \quad \text{R17}$$

$$CH{=}CHCl \rightarrow C_2H_2 + Cl \quad \text{R18}$$

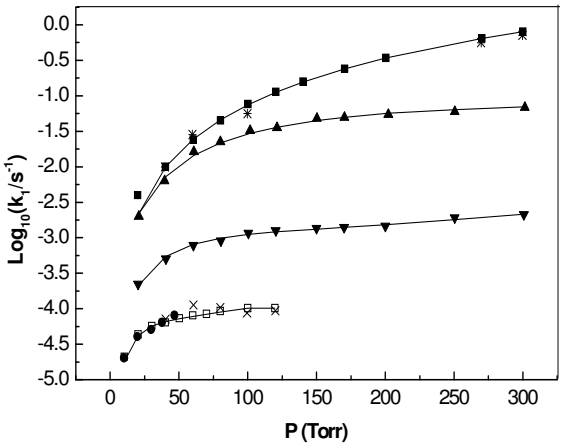

Fig. 3. Dependence of the rate constant for the vinyl chloride formation on the total pressure. Symbols are experimental data. (□) at 849 K in reactor 1, (×) at 849 K in reactor 2, (●) at 849 K without argon, (▼) at 889 K in reactor 1, (▲) at 946 K in reactor 1, (■) at 1064 K in reactor 1, (✳) at 1064 K in reactor 2 without argon. Solid lines are nonlinear least squares fit of equation 1 to the experimental results.

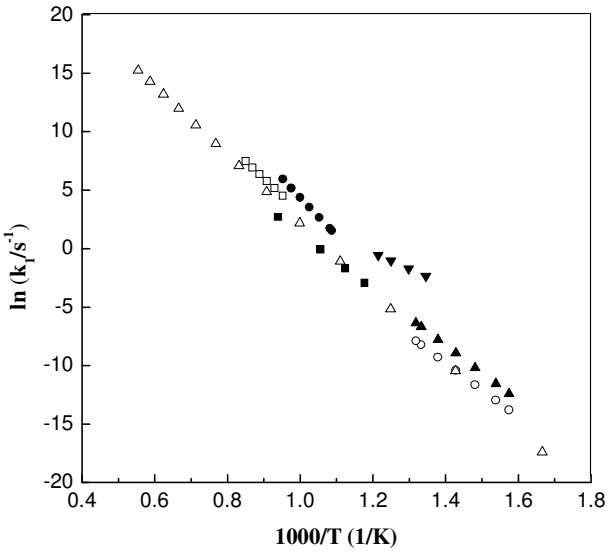

Fig. 4. Dependence of the high-pressure limit of vinyl chloride formation rate constant on the temperature. (■) Our experimental results, (□) from Ref. 14, (▲) from Ref. 5, (●) from Ref. 1(f), (▼) from Ref. 1(g), (○) from Ref. 1(c), (Δ) from Ref. 15.

Table 1. Chordal Rates of Formation of Vinyl Chloride (VC), Ethylene, and Acetylene and Corresponding Rate Constant for the Formation of Vinyl Chloride at Different Conditions in Two Reactors

(T = 849 K, S/V = 9.5 cm^{-1})

P (Torr)	[Reactant] × 10^4 (M)	R_{vc} × 10^8 (M s^{-1})	k_1 × 10^5 (s^{-1})
10	1.2	0.24 (±0.01)	2.1
20	1.5	0.6 (±0.1)	4.3
30	1.9	1.1 (±0.1)	5.6
40	2.3	1.4 (±0.1)	6.3
50	2.7	1.9 (±0.1)	7.2
60	3.1	2.4 (±0.1)	7.9
70	3.5	2.9 (±1.1)	8.3
80	3.7	3.5 (±2.3)	9.1
100	4.6	4.6 (±0.5)	10.0
120	4.7	4.7 (±0.5)	10.2

(T = 849 K, S/V = 17.5 cm^{-1})

P (Torr)	[Reactant] × 10^4 (M)	R_{vc} × 10^8 (M s^{-1})	k_1 × 10^5 (s^{-1})
40	1.9	1.3 (±0.1)	7.0
60	3.1	3.4 (±0.4)	11.0
80	4.1	4.2 (±0.5)	10.0
100	4.6	4.0 (±0.5)	9.0
120	5.1	4.7 (±0.5)	9.0

(T = 889 K, S/V = 17.5 cm^{-1})

P (Torr)	[Reactant] ×10^4 (M)	R_{vc} × 10^7 (M s^{-1})	k_1 × 10^3 (s^{-1})
20	1.8	0.39 (±0.03)	0.2
40	2.4	1.20 (±0.05)	0.5
60	3.3	2.5 (±0.3)	0.8
80	4.1	3.7 (±0.8)	0.9
100	4.2	5.0 (±1.0)	1.2
120	5.9	6.9 (±0.4)	1.2
150	6.2	8.3 (±0.4)	1.3
170	7.2	9.9 (±2.4)	1.4
200	9.0	12.9 (±4.0)	1.4
250	10.3	19.6 (±1.2)	1.9
300	13.9	29.3 (±6.0)	2.1

Table 1. Continued

(T = 946 K, S/V = 9.5 cm^{-1})

P (Torr)	[Reactant] × 10^4 (M)	R_{vc} × 10^5 (M)	R_{C2H2} × 10^7 (M s^{-1})	R_{C2H4} × 10^9 (M s^{-1})	k_1 × 10^2 (s^{-1})
20	1.7	0.043 (±0.007)	-	-	0.2
40	2.6	0.20 (±0.02)	-	-	0.8
60	3.6	0.5 (±0.1)	0.10 (±0.01)	-	1.5
80	4.4	1.0 (±0.4)	0.15 (±0.05)	1.3 (±0.5)	2.2
100	5.5	1.6 (±0.4)	0.2 (±0.1)	1.3 (±0.4)	2.9
120	6.5	2.2 (±0.7)	0.3 (±0.2)	1.4 (±0.2)	3.5
150	7.7	3.2 (±2.0)	0.6 (±0.2)	1.5 (±0.5)	4.2
170	8.6	3.9 (±1.6)	0.7 (±0.2)	1.9 (±0.4)	4.6
200	10.1	5.1 (±2.6)	1.5 (±0.5)	2.1 (±0.4)	5.1
250	12.3	6.9 (±3.4)	1.8 (±0.6)	2.5 (±0.3)	5.6
300	14.7	8.9 (±2.0)	6.5 (±0.6)	2.9 (±0.5)	6.0

(T = 1064 K, S/V = 9.5 cm^{-1})

P(Torr)	[Reactant] × 10^4 (M)	R_{vc}×10^4 (M s^{-1})	R_{C2H2}×10^7 (M s^{-1})	R_{C2H4}×10^9 (M $^{-1}$)	k_1 × 10^1 (s^{-1})
20	1.8	0.01 (±0.01)	0.1 (±0.0)	5.7 (±0.3)	0.1
40	2.9	0.03 (±0.01)	0.3 (±0.1)	6.2 (±0.1)	0.1
60	4.0	0.10 (±0.01)	0.4 (±0.1)	6.5 (±0.2)	0.2
80	5.1	0.23 (±0.05)	0.6 (±0.1)	6.9 (±0.5)	0.4
100	6.2	0.5 (±0.1)	1.0 (±0.1)	7.1 (±0.4)	0.8
120	7.4	0.8 (±0.2)	2.7 (±1.2)	7.6 (±0.7)	1.1
140	8.4	1.3 (±0.6)	4.9 (±1.3)	8.1 (±0.2)	1.6
170	10.1	2.4 (±1.3)	7.9 (±1.4)	8.4 (±0.4)	2.4
200	11.8	4.0 (±2.6)	10.7 (±3.0)	8.6 (±0.8)	3.4
270	15.6	10.0 (±1.0)	15.3 (±6.0)	9.8 (±0.4)	6.4
300	17.2	13.7 (±8.7)	14.3 (±8.1)	10.1 (±0.5)	8.0

(T = 1064 K, S/V = 17.5 cm^{-1})

P (Torr)	[Reactant] × 10^4 (M)	R_{vc} × 10^3 (M s^{-1})	R_{C2H2} × 10^7 (M s^{-1})	R_{C2H4} × 10^9 (M s^{-1})	k_1 × 10^1 (s^{-1})
40	3.7	0.004 (±0.002)			0.1
60	3.9	0.002 (±0.001)			0.3
100	5.8	0.03 (±0.01)	1.7 (±0.4)	9.1 (±0.5)	0.5
270	20	1.1 (±0.1)	14.3 (±5.1)	12.1 (±1.2)	5.5
300	23	1.6 (±0.7)			6.9

Table 2. Calculated Parameters Used in Troe Method to Estimate the Limiting High-Pressure Unimolecular Rate Constant for Reaction R1

T (K)	S_k	B_k	F^{SCC}
849	7.87	12.40	0.237
889	8.10	12.49	0.230
946	8.38	12.48	0.225
1064	8.92	12.44	0.219

for the activation energy of reaction R17, while Schneider and Wolfrum [23] reported a value of 55.7 kJ mol^{-1} for the activation energy of this reaction. Reaction R19 is a barrier less step [24]. To estimate the contribution of these reactions in the formation and consumption of acetylene more study is needed.

THEORETICAL APPROACH

For a better understanding of the mechanism of the pyrolysis of EDC, *ab initio* molecular orbital calculations were carried out to investigate the chemical dynamics of different path ways in this system. RRKM method and transition state theory were used to calculate the relevant rate constants.

Ab Initio Calculations

In this study the GaussianW98 [25] program was used to carry out quantum mechanical calculations. All geometries were optimized at the MP2/6-311+G(d,p) and CASMP2/6-311+G(d,p) levels of theory with appropriate active spaces. Potential energy surfaces along the minimum energy paths for reactions R1, R2, R3, R4, and R5 were explored at the MP2/6-311+G(d,p) and CASMP2/6-311+G(d,p) levels. Spin contamination was annihilated by means of mixing HOMO and LUMO states to destroy α-β and spatial symmetries in bond fission reactions.

To obtain more accurate energies along the potential energy surfaces, calculations at the MP4SDTQ [26], CASMP2 [27], QCISD(T) [28] levels were carried out with more flexible basis set 6-311+G(2d,2p). Stationary points were also re-optimized using the DFT method with Becke's three-parameter hybrid functional B3LYP [29]. In MCSCF calculations depending on the nature of the reaction path different numbers of electron and orbital were examined as active space to get better results.

The zero-point energies were determined from the HF harmonic vibrational term values. Calculated vibrational frequencies were scaled by a factor of 0.89 [30].

Calculating the Rate Constants

RRKM calculations were performed to find the rate constant expressions for the unimolecular channels in this system. A general RRKM program by Zhu and Hase [31] was used and modified to calculate the falloff region and high-pressure rate constant k(T). The following expression is normally used to calculate the unimolecular rate constant as a function of pressure [32].

$$k_{uni} = \sigma \frac{\beta_c Z[M]}{h Q_v Q_r} \exp\left(\frac{-E_0}{RT}\right) \Delta E^+ \sum \left[\frac{\{W(E^+_{vr})\} \exp\left(\frac{-E^+}{RT}\right)}{\beta_c Z[M] + k_a(E^*)} \right] \quad (3)$$

Here, σ is the statistical factor, Q_v and Q_r represent the vibrational and rotational partition functions for the reactant, E_0 is the barrier height corrected for zero-point energy, E^+ is the total non-fixed energy of a given transition state, ΔE^+ is the energy increment. $W(E^+_{vr})$ is the sum of vibrational-rotational states of the transition state, $k_a(E^*)$ is the rate constant for conversion of energized molecule to products, β_c is the collisional deactivation efficiency, Z is the collision number, and [M] is the concentration. The rate constant at infinite pressure is calculated according to the following equation [33].

$$k_\infty = \frac{\sigma B_e}{h Q_v Q_r} \exp\left(\frac{-E_0}{RT}\right) \int_{E^+=0}^{\infty} \{W(E^+_{vr})\} \exp\left(\frac{-E^+}{RT}\right) dE^+ \quad (4)$$

No saddle point is expected for dissociation reactions like reactions R3 and R5. To calculate the rate constant according to RRKM method or transition state theory it was necessary to locate the position of the reaction bottleneck for such reactions. To find the position of the bottleneck for these reactions canonical variational transition state theory (CVTST)

and also microcanonical variational RRKM method were used [34]. To find the position of the bottleneck according to CVTST the method described in reference [35] was used. The simple collisional rate constant expression might be written as

$$k(T,R) = P(R)\pi R^2 u_r \exp[-V(R)/k_B T] \quad (5)$$

where P(R) is the product of the quotient of electronic B_e and rotational partition functions B_θ($P(R) = B_e B_\theta$). For association of two radicals (the reverse of dissociation reactions) value of B_e should normally be equal 1/4. B_θ is the quotient of partition functions for hindered and free rotations of the reactants with respect to tumbling or rocking angles, θ. To eliminate the effect of the low vibrational frequencies on the curvature of Arrhenius plot at high temperatures, we did not include those low vibrational frequencies like bending motions in CH_2Cl moiety that do not contribute effectively to the reaction path in the B_θ ratio. u_r is the relative velocity, R is the distance of the two fragments which are separating as the reaction proceeds, and V(R) is the potential energy along the reaction coordinate. The degrees of freedom in the reactant can be divided into conserved modes and transitional modes [36]. Most of the vibrational modes do not change significantly from the reactants to the transition state and only some of them change as reaction proceeds.

Reaction R1

Figure 5 shows the optimized geometries of reactants, transition states, and products of reactions R1, R2, R3, R4, and R5 at the MP2/6-311+G(d,p) level. Potential energy surface for reaction R1 at the MP2/6-311+G(d,p) level of theory is shown in Fig. 6. Total energies of different species at different levels of theory are listed in Table 3. Vibrational term values, rotational constants, and zero point energies for different species are listed in Tables 4 and 5. The corrected potential energy barriers for zero point energies at different levels of theory at zero Kelvin are listed in Table 6.

To calculate the rate constant for reaction R1 according to Eqs. (3) and (4), different values of potential energy barriers calculated at different levels of theory in Table 6 were used. The statistical factor for reaction R1 is 2 and vibrational term values and rotational constants for the reactant and activated complex from Tables 4 and 5 were used. In RRKM calculations, the step size ΔE^+ = 0.4 kJ mol^{-1} up to the E^+ = 10 kJ mol^{-1} at 200 K that increased to a value of 100 kJ mol^{-1} at 3000 K was used. Argon was chosen as bath gas and values of 0.02 to 1.0 was examined for the collision efficiency β_c to check the effect of this parameter in the falloff behavior region [37]. Dependency of k_1 to the pressure according to RRKM theory for three temperatures is shown in Fig. 7, which is compared with our experimental data. Arrhenius plot for reaction R1 from the results at the DFT and QCISD(T) levels of theory is shown in Fig. 8 that compared with the previous results in the literature and also with our experimental data in the present work. According to RRKM method and based on the QCISD(T) and B3LYP results, the Arrhenius expressions for k_1 were found as $k_1 = 7.0 \times 10^{14}$ exp(-275.2 kJ mol^{-1}/RT) s^{-1} from QCISD(T) results and $k_1 = 7.0 \times 10^{14}$ exp(-244.6 kJ mol^{-1}/RT) s^{-1} from B3LYP results. These expressions might be compared with the kinetic parameters calculated from our experimental results using the Troe method, $k_{1,\infty} = 4.2 \times 10^{13}$ exp (-235.7 kJ mol^{-1}/RT). The results for k_1 from B3LYP results are in better agreement with the high pressure limiting values of k_1 calculated by Troe method.

Reaction R2

Reaction R2 is a unimolecular reaction that two possible mechanisms, concerted versus stepwise removal of chlorine atoms, might be proposed for Cl_2 formation. Our calculations showed that the concerted mechanism is more favorable by about 10.0-20.0 kJ mol^{-1}, depending on the level of theoretical calculations. Structure of the transition state for reaction R2 is shown in Fig. 5 and its potential energy surface at the MP2/6-311+G(d,p) level is shown in Fig. 9. Barrier heights, zero point energies, Vibrational term values, and rotational constants are listed in Tables 4 to 6. RRKM method was used to calculate the rate constant of reaction R2 that the results are shown in Fig. 10. In calculating the rate constant for this reaction according to RRKM we used the same procedure that is described in the previous section for reaction R1. According to our calculations at the QCISD(T) level the Arrhenius expression for k_2 were found as $k_2 = 1.6 \times 10^{15}$ exp(-414.3 kJ /RT) s^{-1}. Barton and Howlett in 1949 reported a value of 1×10^{13} s^{-1} for the pre-exponential factor and a value of 301.2 kJ mol^{-1} for the activation energy of this reaction [1(b)], while

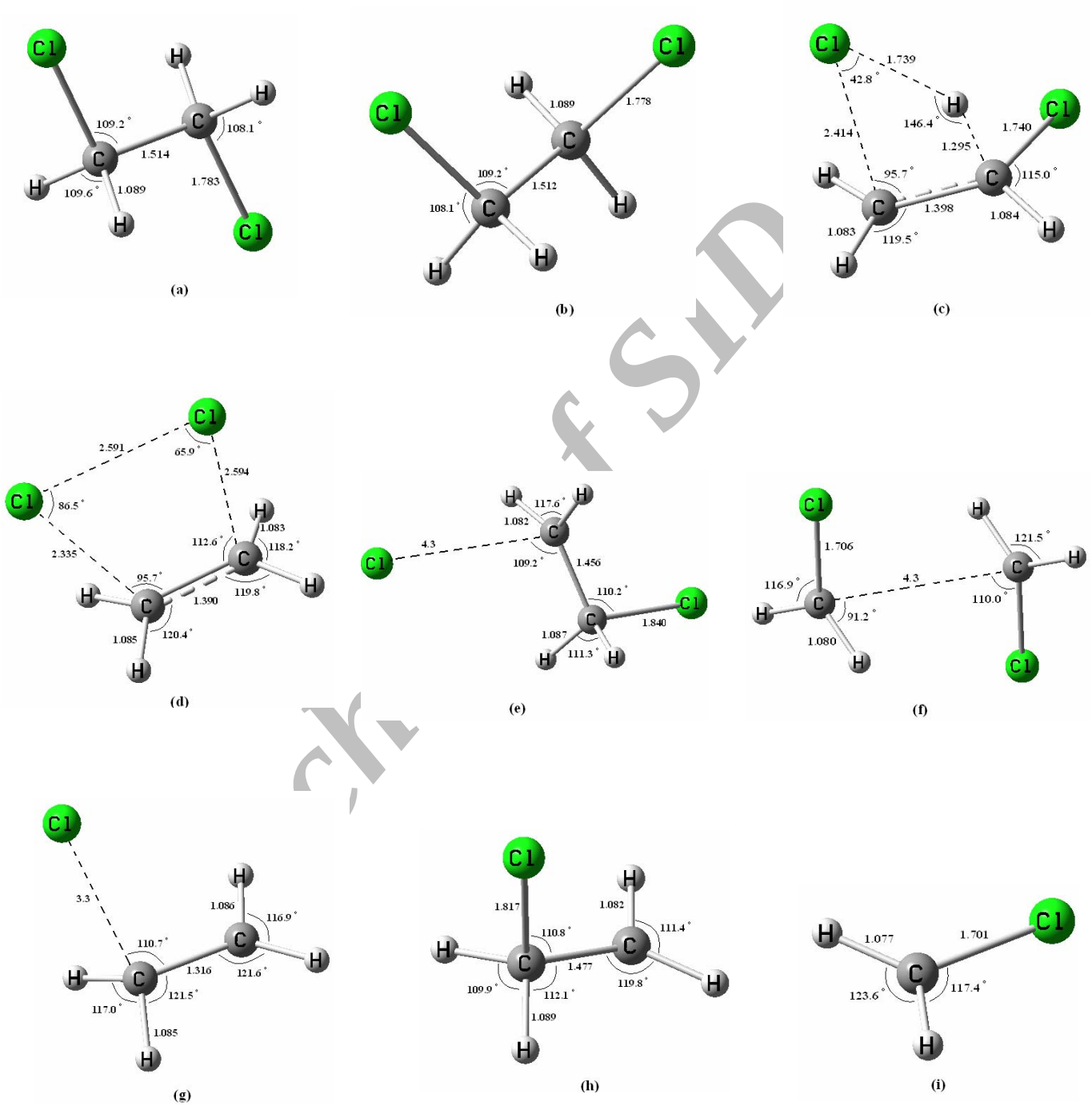

Fig. 5. Optimized geometries of trans- and gauch- 1,2 Dichloroethane (a and b) and the transition states for reactions R1 (c), R2 (d), R3 (e), R4 (g), R5 (f) and the products of reactions R3 (h) and R5 (i) at the MP2/6-311+G(d,p) level.

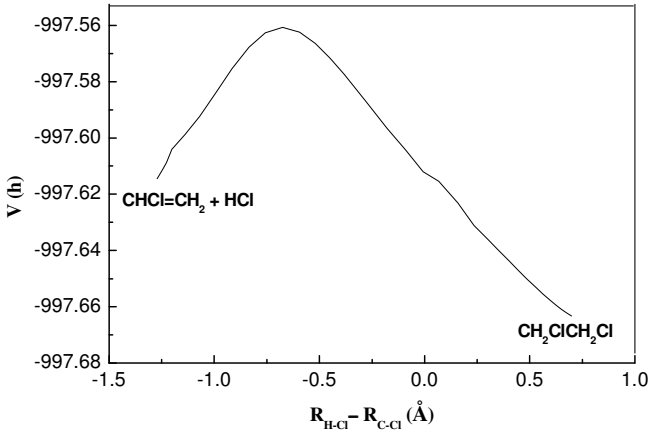

Fig. 6. Potential energy surface for reaction R1 at the MP2/6-311+G(d,p) level of theory.

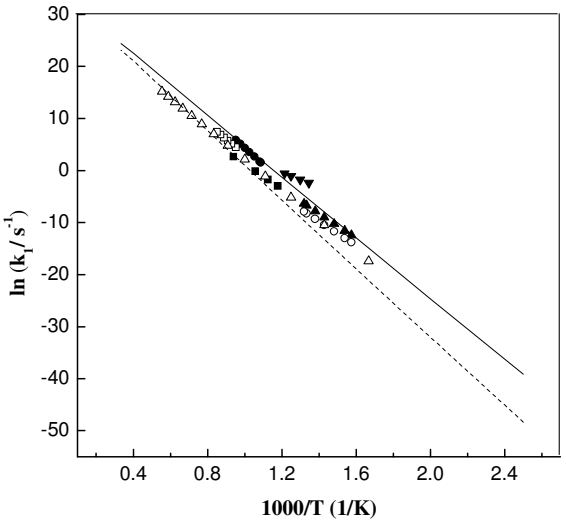

Fig. 8. High-pressure RRKM rate constant of reaction R1 calculated at the B3LYP/6-311+G(2d,2p) level (solid line) and at the QCISD(T)/6-311+G(2d,2p) level (dashed line). (□) from Ref. 14, (▲) from Ref. 5, (●) from Ref. 1(f), (▼) from Ref. 1(g), (○) from Ref. 1(c), (Δ) from Ref. 15, (■) our experimental results.

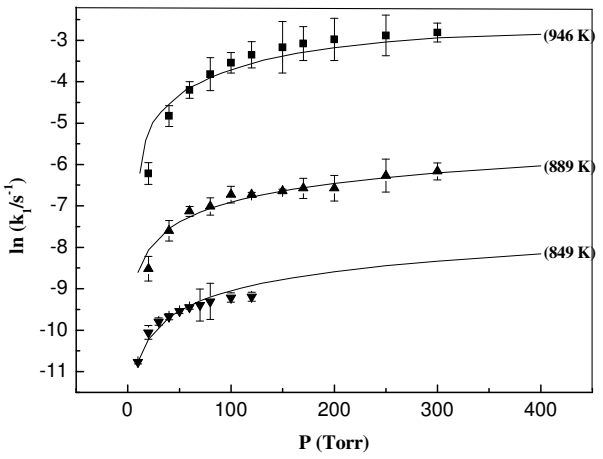

Fig. 7. Fall off behavior of k_1 at three different temperatures. Points are experimental data and solid lines from RRKM calculations.

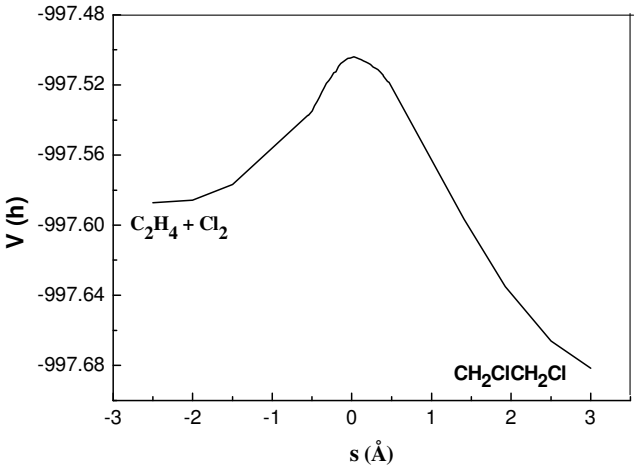

Fig. 9. Potential energy surface for reaction R2 at the MP2/6-311+G(d,p) level of theory.

Table 3. Calculated Total Energies of all Species at Different Level of Theory in amu Along with 6-311+G(2d,2p) Basis Set

	MP2	MP4SDTQ	CASMP2	B3LYP	QCISD(T)
Trans- EDC	-997.74267	-997.81252	-997.89859[a] -997.85612[b]	-999.10761	-997.81285
Gauch- EDC	-997.74033	-997.81015	-997.89034[a] -997.89671[b]	-999.10497	-997.81044
R1 T. S.	-997.63228	-997.70386	-997.72110[a] -997.71656[b]	-999.00978	-997.70511
R2 T. S.	-997.57189	-997.62873		-998.96059	-997.64639
R3 T. S.	-997.60556	-997.68037	-997.75650	-998.98164	-997.68327
R4 T. S.	-537.95639	-538.01220	-537.96587[c]	-538.77494	-538.16590
R5 T. S.	-997.58728	-997.66286	-997.75499	-998.97176	-997.66718
CH_2CHCl	-537.31641	-537.36783	-537.52422	-538.12695	-537.36877
CH_2ClCH_2	-538.00011	-538.05531	-538.00477	-538.81459	-538.05732
CH_2Cl	-498.79364	-498.83143		-499.48588	-498.83359
Cl	-459.60545	-459.62506		-460.16705	-459.62595

[a]CAS(2,2) MP2. [b]CAS(8,8) MP2. [c]CAS(3,3) MP2.

Table 4. Vibrational Term Values in cm^{-1} and Zero-Point Energies in amu for Different Species Calculated at the HF/6-311G(d,p) Level

Species	Frequencies	ZPE
trans-1,2-DCE	2876 2854 2815 2810 1451 1448 1344 1274 1258 1142 1013 1008 791 754 707 293 210 125	0.06023
R1 T. S.	2984 2896 2882 1477 1404 1325 1222 1151 1111 1040 858 743 684 382 365 316 97 1819i	0.05133
R2 T. S.	2946 2918 2857 2839 1476 1396 1200 1164 1041 1037 965 811 510 460 411 250 229 142i	0.05762
R3 T. S.	3011 2901 2897 2835 1475 1425 1260 1241 1098 1030 1029 800 588 215 171 79 60	0.05661
R4 T. S.	2987 2916 2882 2846 1456 1408 1172 1154 1052 819 798 463 294 188 166i	0.04886
R5 T. S.	3014 3013 2885 2883 1391 1387 999 999 787 781 685 491 374 365 103 99 95	0.05210
CH_2CHCl	2950 2915 2864 1550 1347 1261 1026 985 966 703 656 403	0.04512
CH_2CH_2Cl	2956 2861 2861 2811 1451 1411 1266 1232 1054 1012 783 642 574 306 295	0.05507
CH_2Cl	3015 2882 1375 983 798 296	0.02393

Table 5. Rotational Constants for Different Species in GHz

Species	B1	B2	B3
trans-1,2-DCE	29.355	1.515	1.467
gauch-1,2-DCE	10.013	2.261	1.962
R1 T. S	10.351	1.734	1.576
R2 T. S.	4.850	3.270	2.010
R3 T. S	24.485	0.608	0.598
R4 T. S.	27.720	2.340	2.220
R5 T. S	13.592	0.629	0.606
CH_2CHCl	57.247	5.995	5.427
CH_2CH_2Cl	32.920	5.793	5.270
CH_2Cl	274.836	15.848	15.002

Table 6. Barrier Heights Corrected for Zero-Point Energies for Reactions R1, R2, R3, R4, and R5 in kJ mol^{-1}

Method of calculations	R1	R2	R3	R4	R5
MP2/6-311+G(2d,2p)	262.2	441.5	346.4	98.4	375.5
MP4SDTQ/6-311+G(2d,2p)	257.6	475.7	333.4	96.8	360.5
CAS+MP2/6-311+G(2d,2p)	445.3	504.2	363.1	94.6	372.6
B3LYP/6-311+G(2d,2p)	229.2	379.2	317.2	87.7	324.2
QCISD(T)/6-311+G(2d,2p)	259.8	430.2	326.7	90.4	350.0

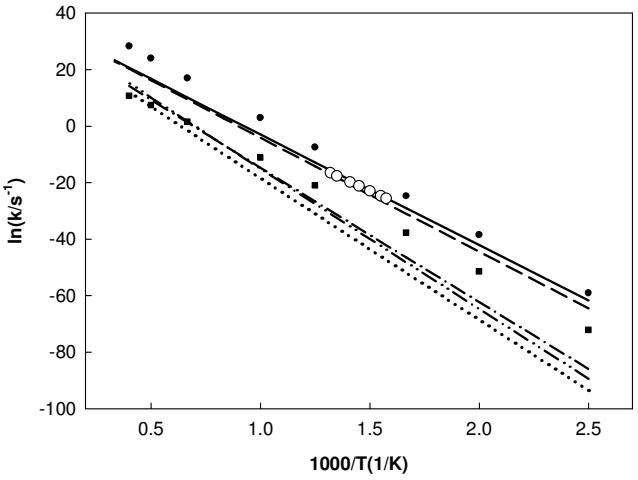

Fig. 10. High-pressure rate constants for reactions R2 and R3 calculated at different levels of theory. Dash-dot-dotted line calculated at the QCISD(T)/6-311+G(2d,2p) level for reaction R2, dotted line from Ref. 4 for reaction R2 calculated at the G3MP2 level, dash-dotted line from Ref. 4 for reaction R2 calculated at the CBS-Q level. Solid line calculated at the B3LYP/6-311+G(2d,2p) level for reaction R3, dashed line calculated at the QCISD(T)/6-311+G(2d,2p) level for reaction R3. (■) from Ref. 1(e) for reaction R3, O from Ref. 5 for reaction R3. (●) from Ref. 17 for reaction R3.

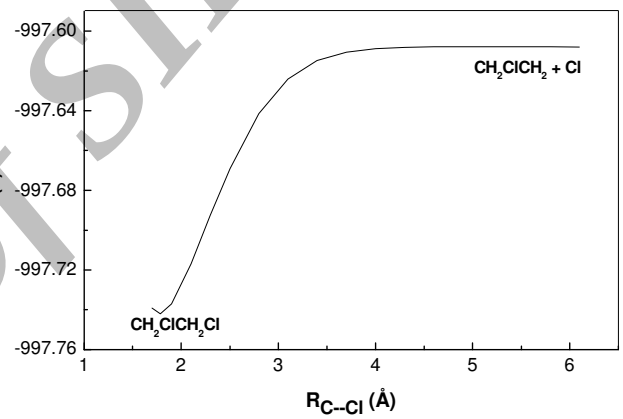

Fig. 11. Potential energy surface for reaction R3 at the CAS(2,2)mp2/6-311+G(d,p) level of theory.

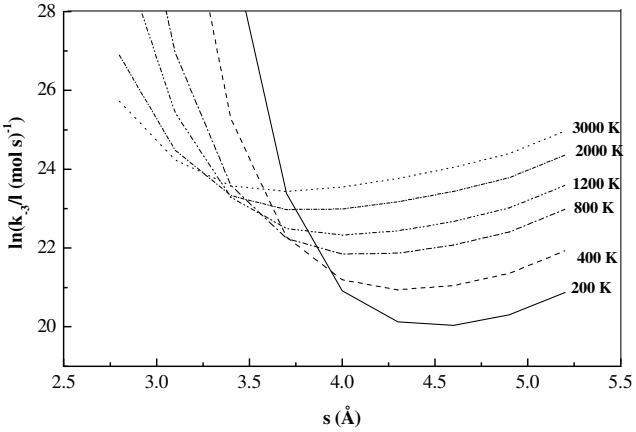

Fig. 12. Calculated rate constant for association reaction of CH_2ClCH_2 + Cl → EDC as a function of C---Cl distance at different temperatures, Eq (5).

zhu and Bozzelli [4] reported the following expression for k_2 at the G3MP2, $k_2 = 7.6 \times 10^{10}\ T^{o.893}\ \exp(-411.7\ kJ\ mol^{-1}/RT)\ s^{-1}$.

Reaction R3

Another possibility for the formation of ethylene as a

Table 7. Microcanonical Variational RRKM Results for Unimolecular Dissociation Reaction $C_2H_4Cl_2$ = CH_2ClCH_2 + Cl

$E(v,j)^a$	$E^{\ddagger}(v,j)^b$	$R^{\ddagger}$ (Å)^c	$E_0{}^d$	$N(v,j)\times10^{10e}$	$G(E^{\ddagger})^f$	$k(E)^g$ (1/s)
353.1	1.7	4.48	365.1	0.6	22	1.1×10^{2}
374.0	23.7	4.16	363.7	1.3	8.2×10^{3}	1.9×10^{4}
394.9	45.1	4.07	363.1	2.6	2.4×10^{5}	2.8×10^{5}
415.8	66.8	3.98	362.0	5.0	3.4×10^{6}	2.0×10^{6}
436.8	88.7	3.91	360.9	9.6	2.9×10^{7}	9.1×10^{6}
457.7	110.0	3.85	360.0	17.8	1.8×10^{8}	3.0×10^{7}
478.6	131.5	3.82	359.5	32.2	9.2×10^{8}	8.5×10^{7}
499.5	152.9	3.79	358.7	57.2	4.0×10^{9}	2.1×10^{8}
520.4	174.5	3.75	357.6	99.6	1.5×10^{10}	4.6×10^{8}
541.4	196.3	3.72	357.1	170.3	5.2×10^{10}	9.2×10^{8}
562.3	218.0	3.69	356.5	286.6	1.6×10^{11}	1.7×10^{9}
583.2	239.9	3.65	355.1	474.7	4.7×10^{11}	2.9×10^{9}
604.1	261.8	3.62	353.5	774.6	1.2×10^{12}	4.8×10^{9}
625.0	283.7	3.59	352.0	1247.0	3.1×10^{12}	7.5×10^{9}
646.0	305.7	3.56	350.8	1980.0	7.5×10^{12}	1.1×10^{10}

[a]Total energy available to the system in kJ mol^{-1}. [b]Transition state energy in kJ mol^{-1}. [c]Position of bottleneck in angstrom. [d]Classical energy difference between the reactant and the transition state in kJ mol^{-1}. [e]Density of states in cm^{-1}. [f]Sum

minor product in this system is unimolecular dissociation reactions R3 followed by reaction R4. Structure of the transition state for reaction R3 is shown in Fig. 5. Potential energy surface for reaction R3 at the CAS(2,2)MP2/6-311+ G(d,p) level of theory is shown in Fig. 11. No saddle point is expected for dissociation reactions like reaction R3. Equation (5) was used to find the position of the bottleneck for reaction R3 using canonical variational transition state theory (CVTST) procedure and also microcanonical variational RRKM method were used.

To find the position of the bottleneck for reaction R3 by means of Eq. (5), the reverse of reaction R3, CH_2ClCH_2 + Cl $\rightarrow$ CH_2ClCH_2Cl was examined. Using this procedure, rate constant for reaction R3 has been calculated at different temperatures from 200 K-3000 K and for the values of $R_{C\text{-}Cl}$ bond length between 2.5-6 Å. The results from CAS(2,2)MP2 surface was used to calculate the rate constant for reaction R3 as a function of C-Cl distance and temperature. The results are shown in Fig. 12. As shown in Fig. 12, on the CASMP2 surface the bottleneck for the rate of reaction R3 was found at C-Cl bond distance of 4.8 Å at lower temperatures. This value decreased to a value of 3.8 Å as temperature approaches to 3000 K.

In the present study, we also performed microcanonical variational RRKM calculations to locate the position of the transition state for reaction R3 at different temperatures. A general RRKM program from Zhu and Hase [31] was used to carry out this kind of calculations. CASMP2 potential energy surface was used to calculate the sum of states of the system at different C-Cl bond lengths for dissociation of C-Cl bond. The RRKM program searches for the minimum in the sum of states versus reaction coordinate as a function of available energy to locate the position of the bottleneck. The results are shown in Table 7. According to RRKM calculations, the position of the bottleneck for reaction R3 was found to be 4.48 Å of C-Cl bond at lower temperatures (lower energies) that decreased to a value of 3.56 Å at higher energies. To search the bottleneck for reaction R3 along the reaction coordinate, the moments of

inertia and frequencies at each C-Cl bond length along the reaction coordinate were calculated. It was found that only two low vibrational term values and two moments of inertia were changing significantly with changing the C-Cl bond distance. Therefore, two low vibrational frequencies and two moments of inertia varied at each point along the reaction coordinate. In this kind of calculations, the RRKM program gave the minimum rate constant k(E) in a position along the reaction coordinate that the sum of states is minimum.

To calculate the fall off behavior and high pressure rate constant for reaction R3 according to RRKM program, the vibrational term values and rotational constants from Tables 4 and 5 were used. Values of 0.02 to 1 was used for the collisional deactivation efficiency [37]. According to RRKM theory, the Arrhenius plot for reaction R3 at different levels of theory are shown in Fig. 10 which is compared with the reported results in the literature and calculated rate constant for reaction R2. According to our results at the QCISD level in Fig. 10, the Arrhenius expression for k_3 was found as $k_3 = 6.2 \times 10^{15} \exp(-326.2 \text{ kJ mol}^{-1}/RT) \text{ s}^{-1}$.

Reaction R4

Reaction R4 is a unimolecular reaction for the formation of ethylene that is one of the minor products in this system from C_2H_4Cl radical dissociation, the product of reaction R3. Optimized structure of the transition state for reaction R4 is shown in Fig. 5 and potential energy surface for this reaction at the CAS(3,3)MP2/6-311G(d,p) level is shown in Fig. 13. Our calculations at this level of theory show a saddle point for reaction R4. Vibrational term values and moments of inertia for the transition state of reaction R4 are listed in Tables 4 and 5. TST was used to calculate the high pressure rate constant for reaction R4.

Figure 14 shows the Arrhenius plot for reaction R4 at high pressure limit, which is in good agreement with the results reported by Barat and Bozzelli [7]. According to our results the Arrhenius parameters for reaction R4 were found as $k_4 = 1.13 \times 10^{14} \times \exp(-98.6 \text{ kJ mol}^{-1}/RT) \text{ s}^{-1}$.

Reaction R5

Reaction R5 is a unimolecular dissociation reaction in which carbon-carbon bond in EDC is breaking. This reaction is not important in this system at lower temperatures, while

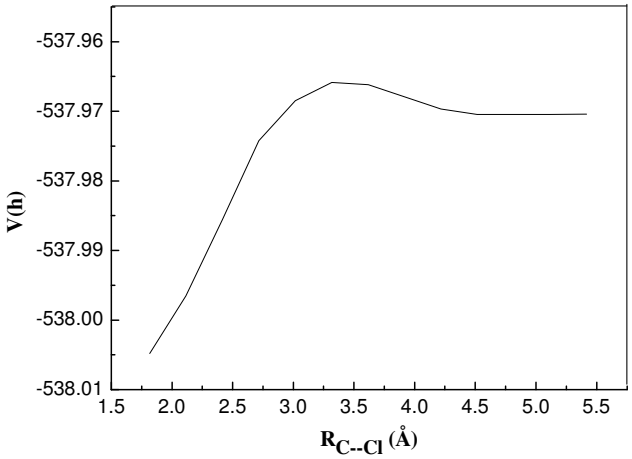

Fig. 13. Potential energy profile for reaction $C_2H_4Cl = C_2H_4 + Cl$ explored at the CAS(3,3)MP2/6-311G(d,p).

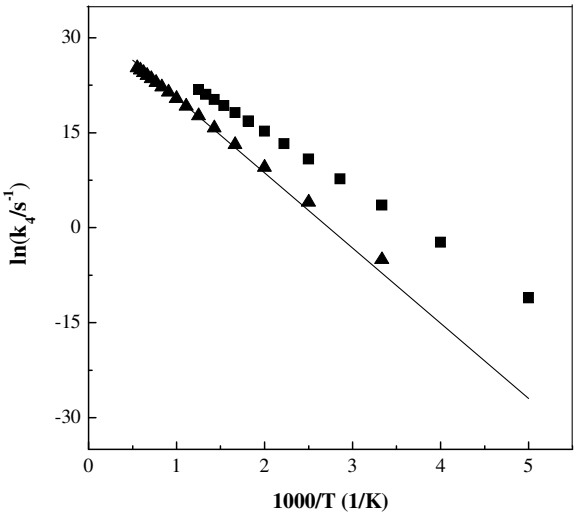

Fig. 14. Arrhenius plot for reaction R4. Solid line from RRKM calculations according to the QCISD/6-311+G(2d,2p) results, (▲) from Ref. 7, and (■) from Ref. 8.

increasing the temperature or the number of chlorine atoms in this molecule increasing the role of C-C bond cleavage. The structure of the transition state for this reaction is shown in Fig. 5 and potential energy surface for this reaction at the CAS(2,2)MP2/6-311G(d,p) level of theory is shown in Fig. 15. No saddle point is expected for dissociation reactions like

reaction R5. To find the position of the bottleneck for reaction R5 canonical variational transition state theory (CVTST) and also microcanonical variational RRKM method were used. The procedures used for these methods are described in previous sections.

According to Eq. (5), rate constant for reaction R5 has been calculated at different temperatures from 200-3000 K and for values of R_{C-C} between 2.5-6 Å. The results from CAS(2,2)MP2 method in Fig. 15 was used to calculate the rate constants for reaction R5 as a function of C-C distance and temperature (Fig. 16). As shown in Fig. 16, on the CASMP2 surface the bottleneck for reaction R5 was found at C-C bond distance of 5.8 Å at lower temperatures which decreased to a value of 3.4 Å as temperature approached to 3000 K.

According to microcanonical variational RRKM calculations, the position of the bottleneck for reaction R5 was found to be 4.31 Å of C-C bond at lower temperatures (lower energies) which decreased to a value of 3.5 Å at higher energies. The results are shown in Table 8. To search the bottleneck for reaction R5 along the reaction coordinate, the moments of inertia and frequencies at different C-C bond length along the reaction coordinate were calculated. It was found that only two low vibrational term values and two moments of inertia were changing significantly by changing the C-C bond length.

The data from microcanonical variational RRKM calculations were used for the bottleneck to calculate the high pressure rate constant for this reaction. The parameters used to calculate the rate constant for reaction R5 according to RRKM method are shown in Tables 4 and 5. Arrhenius plot for reaction R5 is shown in Fig. 17. Arrhenius parameters for reaction R5 from QCISD and B3LYP results are found as $k_5 = 1.7 \times 10^{16} \exp(-364.6 \text{ kJ mol}^{-1}/RT) \text{ s}^{-1}$ and $k_5 = 1.8 \times 10^{16} \exp(-339.1 \text{ kJ mol}^{-1}/RT) \text{ s}^{-1}$, respectively.

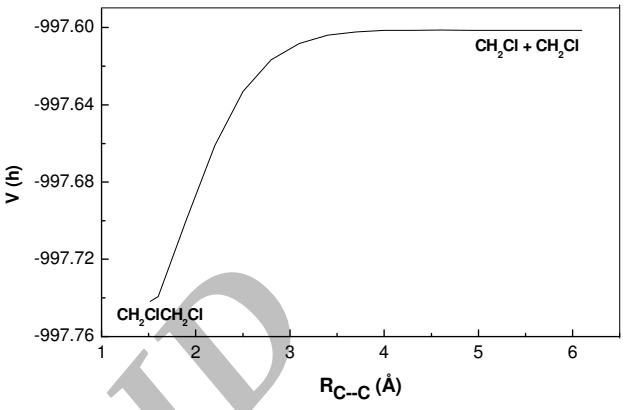

Fig. 15. Potential energy surface for reaction R5 calculated at the CAS(2,2)mp2/6-311+G(d,p) level of theory.

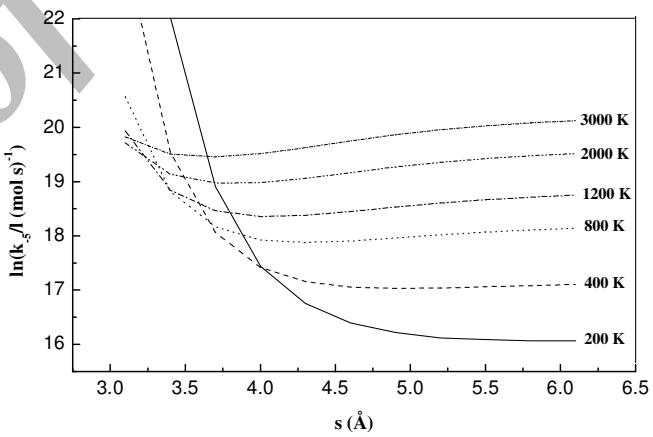

Fig. 16. Calculated rate constant for association reaction of $2CH_2Cl \rightarrow$ EDC as a function of C---C distance at different temperatures, Eq. (5).

DISCUSSION

Pyrolysis of EDC over the temperature range of 849-1064 K is studied experimentally to investigate the pressure dependency of vinyl chloride. We also measured the average rate of formation of ethylene and acetylene to investigate the mechanism of formation of these two products in this system. The Troe method was used to calculate the pressure dependency of vinyl chloride formation. In this system, two paths could be proposed for the formation of vinyl chloride, *via* a four center HCl elimination (reaction R1), or stepwise elimination of chlorine atom and hydrogen atom (reactions R3 and R10). Two paths also exist for the formation of ethylene, reaction R2 for four center Cl_2 elimination and reactions R3 and R4 for stepwise Cl elimination.

To investigate the mechanism of formation of vinyl chloride and ethylene we performed *ab initio* calculations for reactions R1, R2, R3, R4, and R5. Our results showed that

Table 8. Microcanonical Variational RRKM Results for Unimolecular Dissociation Reaction $C_2H_4Cl_2 = CH_2Cl + CH_2Cl$

$E(v,j)^a$	$E^{\ddagger}(v,j)^b$	$R^{\ddagger}$ (Å)^c	$E_0{}^d$	$N(v,j) \times 10^{12e}$	$G(E^{\ddagger})^f$	$k(E)^g$ (1/s)
369.9	1.0	4.31	393.8	0.01	11	29.7
389.9	21.6	4.02	392.9	0.02	8067	1.1×10^{4}
410.9	43.1	3.89	392.2	0.04	3.5×10^{5}	2.4×10^{5}
431.8	64.2	3.82	391.3	0.08	5.7×10^{6}	2.1×10^{6}
452.7	85.5	3.77	390.7	0.15	5.7×10^{7}	1.1×10^{7}
473.6	106.9	3.72	390.2	0.28	4.1×10^{8}	4.3×10^{7}
494.5	128.3	3.67	389.9	0.50	2.3×10^{9}	1.3×10^{8}
515.5	149.7	3.63	389.2	0.87	1.1×10^{10}	3.6×10^{8}
536.4	171.2	3.59	387.7	1.50	4.0×10^{10}	8.5×10^{8}
557.3	192.7	3.55	387.0	2.53	1.5×10^{11}	1.8×10^{9}
578.2	213.3	3.53	386.5	4.21	4.0×10^{11}	3.4×10^{9}
599.1	234.5	3.52	386.3	6.90	1.4×10^{12}	6.2×10^{9}
620.1	255.8	3.5	386.1	11.13	3.9×10^{12}	1.0×10^{10}
641.0	277.0	3.48	385.9	17.74	1.0×10^{13}	1.7×10^{10}
661.9	298.4	3.46	385.7	27.91	2.5×10^{13}	2.7×10^{10}

[a]Total energy available to the system in kJ mol^{-1}. [b]Transition state energy in kJ mol^{-1}. [c]Position of bottleneck in angstrom. [d]Classical energy difference between the reactant and the transition state in kJ mol^{-1}. [e]Density of states in cm^{-1}. [f]Sum of states.

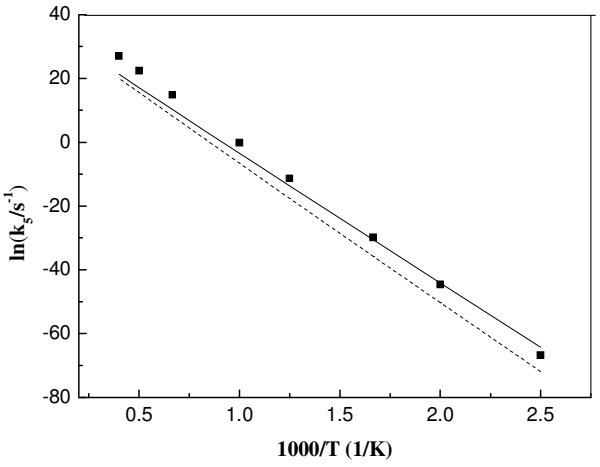

Fig. 17. Arrhenius plot for reaction R5 from RRKM calculations using QCISD/6-31G+(2d,2p) results (dashed line) and B3LYP/6-31G+(2d,2p) results (solid line). Points are from Ref. 17.

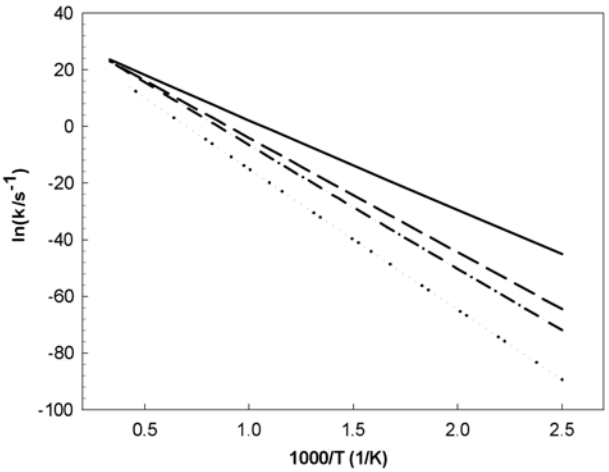

Fig. 18. Comparison between the rate constants of different channels. Solid line for k_1, dotted line for k_2, dashed line for k_3, dashed-dotted line for k_5.

vinyl chloride formed in reaction R1 is the major channel and for ethylene formation all reactions R2, R3, and R4 are the contributors. In Fig. 10 are compared the rate constant for reaction R2 with the rate constant for reaction R3. As shown in Fig. 10, the major path for the formation of ethylene should be stepwise chlorine atom elimination. Analyzing the experimental results for the formation of acetylene indicates that some bimolecular reactions should also be involved in the formation of acetylene and more study is needed to characterize its behavior. We were also interested to investigate the kinetics of reaction R5, theoretically. Although, we detected chloromethane and dichloromethane as minor products in our experimental study, it was difficult to measure these products quantitatively, due to their retention time in GC Our results showed that reaction R5 should be more important than reaction R2 in this system. In Fig. 18 we compared the rate constants for reactions R1, R2, R3, and R5 to estimate the relative importance of these channels during the pyrolysis of EDC. According to Fig. 18, the decomposition of EDC proceeds by 99.90 *% via* reaction R1, 6×10^{-6}*% via* reaction R2, 0.08*% via* reaction R3, and 0.01*% via* reaction R5.

REFERENCES

[1] a) K.E. Howlett, D.H.R. Barton, Trans. Faraday Soc. 45 (1949) 735; b) D.H.R. Barton, K.E. Howlett, J. Chem. Soc. (1949) 155; c) D.H.R. Barton, J. Chem. Soc. London (1949) 148; d) G. Huybrechts, Y. Hubin, B. van Mele, Int. J. Chem. Kinet. 24 (1992) 671; e) A.G. Borsa, A.M. Herring, J.T. McKinnon, R.L. McCormick, G.H. Ko, Ind. Eng. Chem. Res. 40 (2001) 2428; f) N.N. Buravtsev, A.S. Grigorev, O.A. Zaidman, Y.A. Kolbanovskii, M.Y. Markelov, M.N. Sadogurskii, Y. A. Treger, Khim. Fiz. 11 (1992) 210; g) M. Kitabatake, T. Onouchi, Kogyo Kagaku Zasshi 65 (1962) 931.

[2] K.A. Holbrook, R.W. Walker, W.R. Watson, J. Chem. Soc. B (1971) 577.

[3] H. Cardy, C. Larrieu, M. Chaillet, J. Ollivier, Chem. Phys. 169 (1993) 305.

[4] L. Zhu, W. Bozzelli, Chem. Phys. Let. 357 (2002) 65.

[5] K.E. Howlett, Trans. Faraday Soc. 48 (1952) 25.

[6] M. Salouhi, P.M. Marquaire, G.M. Come, J. Chem. Phys. 69 (1999) 797.

[7] R.B. Barat, W. Bozzelli, J. Phys. Chem. 96 (1992) 2494.

[8] V.D. Knyazev, I.J. Kalinovski, I.R. Slagle, J. Phys. Chem. A 103 (1999) 3216.

[9] J.A. Incavo, Ind. Eng. Chem. Res. 35 (1996) 931.

[10] G.J. Martens, G.H. Huybrechts, J. Chem. Phys. 43 (1965) 1845.

[11] S.H. Mousavipour, V. Saheb, S. Ramazani, J. Phys. Chem. 108 (2004) 1946.

[12] B-H. Song, B-S. Choi, S-Y. Kim, J. Yi, Hwahak Konghak 39 (2001) 481.

[13] B-S. Choi, J.S. Oh, S-W. Lee, H. Kim, J. Yi, Ind. Eng. Chem. Res. 40 (2001) 4040.

[14] B. Rajakumar, K.P.J. Reddy, E. Arunan, J. Phys. Chem. A 106 (2002) 8366.

[15] B. Rajakumar, E. Arunan, Phys. Chem. Chem. Phys. 5 (2003) 3897.

[16] J.C. Hassler, D.W. Setser, R.L. Johnson, J. Chem. Phys. 45 (1966) 3231. J.C. Hassler, D.W. Setser, J. Chem. Phys. 45 (1966) 3246.

[17] S.B. Kara, S.M. Senkan, Ind. Eng. Chem. Res. 27 (1988) 447.

[18] J.A. Seetula, J. Chem. Soc. Faraday Trans. 94 (1998) 1933.

[19] J. Cioslowski, G. Liu, D. Moncrieff, J. Am. Chem. Soc. 119 (1997) 11452.

[20] S.H. Mousavipour, P.D. Pacey, J. Phys. Chem. 100 (1996) 3573.

[21] J. Troe, Ber. Bunsenges, Phys. Chem. 87 (1983) 161 and 177.

[22] J.A. Manion, R. Louw, J. Chem. Soc. Perkin Trans. 2 (1988) 1547.

[23] M. Schneider, J. Wolfrum, Ber. Bunsenges. Phys. Chem. 90 (1986) 1058.

[24] R. Atkinson, D.L. Baulch, R.A. Cox, R.F. Hampson, Jr.J.A. Kerr, M.J. Rossi, J. Troe, J. Phys. Chem. Ref. Data 26 (1997) 521.

[25] M.J. Frisch, G.W. Trucks, H.B. Schlegel, G.E. Scuseria, M.A.J. Robb, R.V. Cheeseman, G.J. Zakrzewski, A. Montgomery, Jr.R.E. Stratmann, J.C. Burant, S. Dapprich, J.M. Millam, A.D. Daniels, K.N. Kudin, M.C. Strain, O. Farkas, J. Tomasi, V. Barone, M. Cossi, R. Cammi, B. Mennucci, C. Pomelli, C. Adamo, S.

Clifford, J. Ochterski, G.A. Petersson, P.Y. Ayala, Q. Cui, K. Morokuma, D.K. Malick, A.D. Rabuck, K. Raghavachari, J.B. Foresman, J. Cioslowski, J.V. Ortiz, B.B. Stefanov, G. Liu, A. Liashenko, P. Piskorz, I. Komaromi, R. Gomperts, R.L. Martin, D.J. Fox, T. Keith, M.A. Al-Laham, C.Y. Peng, A. Nanayakkara, C. Gonzalez, M. Challacombe, P.M.W. Gill, B. Johnson, W. Chen, M.W. Wong, J.L. Andres, M. Head-Gordon, E.S. Replogle, J.A. Pople, Gaussian 98, Revision A.3, Gaussian, Inc., Pittsburgh PA, 1998.

[26] R. Krishnan, J.A. Pople, Int. J. Quantum Chem. 14 (1978) 91. R. Krishnan, M.J. Frisch, J.A. Pople, J. Chem. Phys. 72 (1980) 4244.

[27] B.O. Roos, Adv. Chem. Phys. 69 (1987) 399.

[28] J.A. Pople, M. Head-Gordon, K. Raghavachari J. Chem. Phys. 87 (1987) 5968. J. Cizek, Adv. Chem. Phys. 14 (1969) 35. G.E. Scuseria, H.F. Schaefer, III J. Chem. Phys. 90 (1989) 3700.

[29] A.D. Becke, J. Chem. Phys. 98 (1993) 5648.

[30] L.A. Curtiss, K. Raghavachari, G.W. Trucks, J.A. Pople, J. Chem. Phys. 94 (1991) 7221.

[31] L. Zhu, W.L. Hase, *QCPE Program 644*; Quantum Chemistry Program Exchange, Indiana University: Bloomington, IN.

[32] K.A. Holbrook, M.J. Pilling, S.H. Robertson, *Unimolecular Reactions*, 2nd ed., John Wiley & Sons Ltd., Chichester, England, 1996.

[33] D.M. Wardlaw, R.A. Marcus, J. Phys. Chem. 90 (1986) 5383.

[34] W.L. Hase, L. Zhu, Int. J. Chem. Kinetics 26 (1994) 407. S.C. Smith, J. Phys. Chem. 97 (1993) 7034. W.L. Hase, Acc. Chem. Res. 16 (1983) 258.

[35] P.D. Pacey, J. Phys. Chem. A 102 (1998) 8541. S.H. Mousavipour, Z. Homayoon, J. Phys. Chem. A 107 (2003) 8566.

[36] M. Quack, J. Troe, Ber. Bunsen-Gas. Phys. Chem. 78 (1974) 240. D.M. Wardlaw, R.A. Marcus, Chem. Phys. Lett. 110 (1984) 230. J. Chem. Phys. 83 (1985) 3462. S.H. Robertson, A.F. Wagner, D.M. Wardlaw, J. Chem. Phys. 103 (1995) 2917.

[37] L.E.B. Börjesson, S. Nordholm, J. Phys. Chem. 99 (1995) 938.